Isothermal and Scanning Calorimetry Measurements on β-Lactoglobulin

Marion A. M. Hoffmann,[†] Johannes C. van Miltenburg,[‡] Jan P. van der Eerden,[‡] Peter J. J. M. van Mil,*[,†] and Cees G. de Kruif[†]

Netherlands Institute for Dairy Research (NIZO), P.O. Box 20, 6710 BA Ede, The Netherlands, and Debye Institute, Department of Interfaces and Thermodynamics, Utrecht University, Padualaan 8, 3584 CH Utrecht, The Netherlands

Received: January 27, 1997; In Final Form: June 11, 1997[⊗]

The denaturation and aggregation of β-lactoglobulin was studied by isothermal calorimetry. Experiments with several β-lactoglobulin concentrations (15−100 g/L) were performed at temperatures in the range 62−68.5 °C. Even a small change in temperature had a tremendous effect on the shape of the thermograms, depending also very strongly on the β-lactoglobulin concentration used. The measured thermograms were modeled using the kinetic model for the denaturation and aggregation of β-lactoglobulin recently developed by Roefs and De Kruif. In this kinetic model we recognize four consecutive steps: dissociation, unfolding, exchange of disulfide bonds, and aggregation. The numerical calculations yielded results that were in qualitative and quantitative agreement with typical experimental isothermal calorimetry curves. DSC curves and the decrease in concentration of native β-lactoglobulin as a function of time could also be reproduced well. We think that isothermal calorimetry, in combination with this kinetic model, provides a valuable and useful approach to the study of the denaturation and aggregation of β-lactoglobulin and other proteins.

Introduction

Heat treatment is widely used in the processing of whey and whey protein products. Heating induces changes in the whey constituents. Especially the whey proteins are very sensitive to heat treatment, which has a pronounced effect on their structure and their functional properties. The production of whey proteins as a by-product of cheese manufacturing amounts to 5×10^8 kg/yr in the European community. Further utilization of these high-quality food proteins would be stimulated if the effects of heat on these proteins could be better understood and controlled. The thermal behavior of whey proteins is dominated by β-lactoglobulin (β-lg), which is by far the most abundant protein in whey. Therefore, it has been extensively studied;[1] between 1985 and 1995 we found over 200 references addressing the heat denaturation of β-lg. Nevertheless, there is no clear picture of the reactions taking place. Almost invariably experimental results have been interpreted in qualitative and descriptive terms. This study aims at a more quantitative description in connection with a recently developed reaction scheme of the denaturation/aggregation process.

β-lg is a globular protein of 162 amino acid residues with a molecular mass of 18 300 Da. The protein possesses two disulfide bonds (C106−C119 and C66−C160) and one free cysteine (C121).[2] At room temperature and at pH 7.0 the protein mainly exists as a dimer. By increasing the temperature, the equilibrium is shifted toward the monomeric form.[3,4] At temperatures above 40 °C the monomer undergoes small, reversible conformational changes.[4] Upon further heating (above 50 °C) intramolecular bonds are broken and the protein at least partially unfolds. This situation can be pictured as a "molten globule state",[5] with increased exposure of the previously buried inner hydrophobic groups and the thiol group.[6] Hydrophobic interactions between the exposed groups can cause aggregation of the protein molecules while still in the molten globule state. The thiol group in the modified monomer can induce thiol/disulfide exchange reactions, leading to the formation of disulfide-linked aggregates. The disulfide linkage involved in the intermolecular interchange reaction would most likely be the C66−C160 disulfide, which is found in one of the external loops of β-lg. The other disulfide is buried in the inner parts of the protein and is less available for reaction.[2] These aggregation reactions prevent the renaturation of the molecule on cooling.

The most commonly used method in studies of the thermal denaturation of β-lg is differential scanning calorimetry (DSC).[7−12] Thermodynamic analysis of DSC curves representing protein unfolding relies on the assumption that (chemical) equilibrium exists throughout the temperature-induced unfolding process.[13,14] However, at neutral pH denaturation of β-lg is followed by aggregation of the denatured molecules, and the overall reaction becomes totally or partially irreversible, the degree of irreversibility depending on experimental conditions such as scan rate and protein concentration.[11,15] Especially in the case of high levels of irreversibility, the DSC curves cannot be interpreted in terms of equilibrium thermodynamics; only kinetic data can be obtained.[16−18]

In the literature conflicting results exist regarding the kinetics of β-lg denaturation determined by DSC. This reflects the complexity of the process and can partially be ascribed to variations in experimental conditions. To obtain accurate kinetic data, it is necessary to split up the DSC signal into the separate contributions of the denaturation and aggregation process. Only with conditions under which the processes are more or less separated can accurate and reliable kinetic parameters be obtained.[19] However, with the high scan rates used in most

* Corresponding author. Tel +31 318 659585; Fax +31 318 650400; E-mail: pvanmil@nizo.nl.
[†] NIZO.
[‡] Utrecht University.
[⊗] Abstract published in *Advance ACS Abstracts,* August 1, 1997.

S1089-5647(97)00320-9 CCC: $14.00

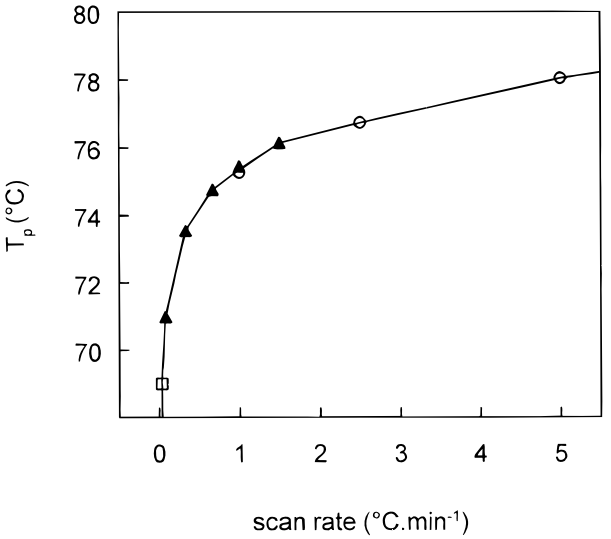

Figure 1. T_p determined with DSC for 50 g/L β-lg as a function of scan rate. To cover a wide range of scan rates, we used three different calorimeters: (○) a Perkin-Elmer DSC7 (50 μL, 60−600 °C/h), (▲) a Hart Scientific DSC 4207 (700 μL, 5−90 °C/h), and (□) an adiabatic calorimeter (≈2 °C/h). With the Perkin Elmer DSC 7 and the Hart Scientific DSC 4207, T_p was determined from three replicate runs and did not vary by more than 0.5 °C.

DSC studies (rates above ±1 °C/min) only one peak is observed with too little fine structure for deriving reliable kinetic data. Since denaturation is an endothermic process, while aggregation is exothermic, the two processes may give rise to only one peak in the thermogram, which is thus difficult to analyze. Nevertheless, it is desirable to separate the various contributions to the overall process. Initially, we tried to separate the processes in time by using very low scan rates in DSC. To cover a wide range of scan rates, we used two different calorimeters: a Perkin-Elmer DSC 7, which is convenient for high scan rates because of low thermal inertia, and a Hart Scientific DSC 4207, which is preferable with lower scan rates, due to the high stability, higher sensitivity, and the larger size of its calorimetric ampules. Figure 1 shows the temperatures of maximum excess heat capacity (T_p) obtained with 50 g/L β-lg as a function of scan rate. Although the peak became more asymmetrical with decreasing scan rate, in all cases only one peak was seen (even at the lowest scan rate of 5 °C/h). We also used an adiabatic setup, which enabled us to heat the β-lg solution at a rate as low as 2 °C/h. With this calorimeter a very asymmetric peak was obtained with a shoulder at ≈60 °C, indicating that indeed more processes are occurring and that these processes could be, at least partially, separated by lowering the scan rate. Further experimental details on these DSC experiments will be given elsewhere.[20] From Figure 1 it can be seen that on lowering the scan rate below ≈1 °C/min T_p becomes strongly dependent on scan rate, indicating that the reactions are strongly kinetically controlled. At temperatures below 70 °C the processes involved in the denaturation and aggregation of β-lg take place on a much larger time scale than a DSC experiment, and therefore it will be virtually impossible to derive correct kinetic parameters from DSC thermograms.

In order to solve the problem, we reverted to true isothermal calorimetry; i.e., we measured the heat exchange of a sample with its surroundings at a fixed temperature. Isothermal calorimetry has the advantage that, as the temperature is kept constant during an experiment, one fewer variable is introduced, thus simplifying the interpretation of data.[21] Compared with conventional DSC, the method is more time-consuming because in order to establish the temperature dependence of the rate constants, several experiments at different temperatures have to be performed. But especially in the case of complex reactions, where the order or even the reaction mechanism is unknown, isothermal calorimetry is very useful because it gives more insight into the mechanism and leads to more accurate kinetic parameters.

Isothermal microcalorimetry has found a wide range of applications, i.e., in pharmaceutical industry,[22] life science research,[23−25] and chemical industry.[26,27] However, as far as we know, isothermal calorimetry has not been used in studying the thermal denaturation of β-lg or other proteins. The aim of this study was to investigate the potential for isothermal microcalorimetry in the study of the thermal denaturation and aggregation of β-lg. Several β-lg concentrations were measured at different temperatures in the temperature range 62−68.5 °C. The results were interpreted in terms of a kinetic model for the denaturation and aggregation of β-lg recently developed by Roefs and De Kruif.[28,29]

Theory

In isothermal calorimetry the rate of heat production is measured directly. For any reaction A → B the instantaneous heat production or heat flow (dQ/dt, in J s^{-1}) at time t is proportional to the rate of reaction of A: $dQ/dt = VQ_{mol}(-d[A]/dt)$, where Q_{mol} is the heat evolved per mole of reactant A and V is the reaction volume.

In the kinetic model used the denaturation and aggregation of β-lg is described by analogy with a radical-addition polymerization reaction.[28] The reaction scheme contains an initiation, a propagation, and a termination step, and the free thiol group of β-lg plays the role of the radical. The initiation step consists of (a number of) reversible reactions, in which the β-lg dimer is split into two monomers, followed by an irreversible step, which is the real initiation reaction. This latter reaction is a first-order reaction (rate constant k_1, molar heat Q_1) in which the conformation of native β-lg (B) is transformed in such a way that the free thiol group (C121) becomes reactive (B*). In the propagation step (rate constant k_2, molar heat Q_2) the reactive thiol group of B* reacts via a thiol/disulfide exchange reaction with the C66−C160 disulfide bond on the outer surface of a nonreactive β-lg molecule. An intermolecular disulfide bond is formed, and a new reactive thiol group becomes accessible; so the propagation step can be repeated many times, leading to the formation of (linear) aggregates. The polymerization process stops when in the termination step (rate constant k_3, molar heat Q_3) two reactive intermediates react with each other, forming a polymer (B_p) without a reactive thiol group. In this model the monomers are linearly linked, but the polymeric aggregates are not stiff rods and may even obtain a spherical shape.

Roefs and De Kruif[28] have already shown that on assuming a steady-state situation the overall decrease in concentration of native β-lg follows a reaction of order 1.5. By applying an overall reaction of order 1.5, they and Hoffmann et al.[29] were able to give a good description of the decrease in concentration of native β-lg on heating and the scattering intensity measured during *in situ* light-scattering experiments. By the use of isothermal calorimetry experiments, we modeled the rate of the

individual steps in the reaction scheme. Scheme 1 gives an overview of the different reaction steps.

SCHEME 1

dissociation:	$B_2 \rightarrow 2B$	k_{diss}	Q_{diss}
initiation:	$B \rightarrow B^*_1$	k_1	Q_1
propagation:	$B + B^*_1 \rightarrow B^*_2$	k_2	Q_2
	$B + B^*_2 \rightarrow B^*_3$	k_2	Q_2
	$B + B^*_i \rightarrow B^*_{i+1}$	k_2	Q_2
termination:	$B^*_i + B^*_j \rightarrow B_{p,i+j}$	k_3	Q_3

One of the complications in examining the denaturation and aggregation of β-lg is the temperature-dependent dissociation of β-lg dimers. Therefore, in our calculations the dissociation of the β-lg dimer (B_2) into the monomers (B) was treated as an extra reaction step (rate constant k_{diss}, molar heat Q_{diss}). The dissociation of native β-lg dimer to monomer was considered an irreversible reaction. We realize that this may be too simple a representation, but in order to keep the scheme as simple as possible, we omitted the association step. We used an (apparent) equilibrium constant K_{eq}, which gave the concentrations of B and B_2 at time zero (i.e., after 20 min temperature equilibration in the isothermal calorimeter). In the literature several values of K_{eq} for β-lg A or β-lg B can be found.[3,30,31] However, most studies were performed at relatively low temperatures (5−25 °C) and at ionic strength 0.1, so an extrapolation had to be made. In the calculations we used $K_{eq} = 3 \times 10^{-3}$ mol L^{-1} at 65 °C. The temperature dependence of K_{eq} was calculated using the van't Hoff relation ($d(\ln K_{eq})/dT = \Delta H/(RT^2)$) with $\Delta H = 65$ kJ mol^{-1}.[30]

In our calculations Q_{diss}, Q_1, and Q_2 were assumed to be endothermic whereas Q_3 was taken as exothermic. This seems reasonable because in the first three reactions bonds are broken (dissociation and initiation) or both broken and formed (propagation step), whereas the termination step only leads to the formation of bonds. From the literature no indications of the values of the rate constants and the reactions heats could be obtained (as the values reported in literature are the sum of several reaction steps), but we chose realistic values, i.e., no larger rate constants than diffusion limitation would allow.

The differential equations describing the production of reactants were solved numerically. For computational reasons the maximum chain length (i) of the active polymers (B^*_i) formed in the propagation step is taken to be P_{max}. In the termination step these active polymers can combine to a inactive polymer $B_{p,i}$ of a maximum chain length of $i = 2P_{max}$. For each time step Δt the concentration of B (native β-lg monomer), B_2 (native β-lg dimer), B^*_i (activated polymer with a chain length i, $1 \le i \le P_{max}$), and $B_{p,i}$ (inactive polymer with a chain length i, $2 \le i \le 2P_{max}$) was determined. This was repeated until the final time t_{end} was reached. For all calculations it was checked that the value chosen for P_{max} was large enough and that the time interval Δt was small enough so as to make the results independent of P_{max} and Δt.

Experimental Section

Materials. The β-lg used in the experiments was a purified β-lg sample, containing the genetic variants A and B (in a nearly 1:1 ratio), which was prepared at NIZO from whey, basically following the procedure of Maubois et al.[32] The sample contained about 92% β-lg, 2% α-lactalbumin, 2% non-protein nitrogen material, and 2.1% ash (including 0.73% Na^+, 0.02% K^+, 0.12% Ca^{2+}, and 0.008% Mg^{2+}) on a dry mass basis. It contained 4.0% moisture.[29]

Sample Preparation. The β-lg powder was dissolved in double-distilled water in a concentration range between 15 and 100 g of dry matter/L and stirred for 2 h. The pH in these solutions varied between 6.75 (100 g/L) and 7.0 (15 g/L). After preparation the solutions were filtered (0.1 μm Millipore low-protein-binding filter).

At the beginning of an experiment 2.50 ± 0.01 g of protein solution was placed into a stainless steel sample vessel (4 mL), which was sealed with a Teflon washer and a stainless steel screw cap. The reference vessel contained the same amount of double-distilled water. Both the sample and reference vessels were carefully weighed before and after the experiment to check the occurrence of any leakage. Measurements in which mass losses larger than 1.0 mg had occurred were discarded.

Isothermal Calorimetry Measurements. The microcalorimeter system used was the 2277 thermal activity monitor (TAM), Thermometric AB (formerly LKB), Sweden.[33] The system consists of a 25 L thermostated water bath, which can hold up to four independently operating calorimeter units. Each calorimeter unit (measuring cylinder) contains a sample and a reference vessel and registers the difference in heat flow between the sample and the reference vessel, which corresponds to the heat generated in the sample. Using this twin principle, effects not due to the sample are minimized. The calorimeters were electrically calibrated using an internal or an external calibration heater (which was positioned in the sample vessel). Analysis of the time decay of the calibration curves indicated in all cases a single-exponential decay with a time constant of 290 ± 20 s. This time constant was very small on the time scale of the reactions studied, so no dynamic correction had to be made for the finite time response of the calorimeter.[23,33] In the TAM, experiments can be performed in the temperature range 20−80 °C. In our study experiments were performed at temperatures between 62 and 68.5 °C. The apparatus was placed in a temperature-controlled room, where the temperature was kept at 17 °C and varied by less than 1 °C. Under these conditions the temperature in the water bath remains constant within 2×10^{-4} °C.[33] Two measuring cylinders were available in this study, so two experiments were made simultaneously at each temperature. After preparation of the sample and reference vessels the ampules were lowered slowly and smoothly into the measuring cylinder by means of an ampule lifter. Before reaching the measuring positions, the vessels had to reach the experimental temperature. This was achieved by equilibrating the vessels 20 min in the temperature equilibration position. (During several subsequent measurements the reference was left in the measuring position.) After this time the vessels were lowered into the measurement position, and the computer program and the monitoring of the heat flow signal were started. This time was taken as $t = 0$, but in kinetic calculations the time was adjusted for the equilibration time. The heat flow signal (dQ/dt, in microwatts) was monitored as a function of time for about 42 h. By integrating the heat flow curve over a specific time interval, the heat (Q, in joules) evolved or absorbed was obtained. Exothermic signals were given positive values.

Results and Discussion

Typical Curves and Correction of the Thermograms. Figure 2 shows typical thermograms measured at 65 °C for a blank measurement and for two 100 g/L β-lg solutions in stainless steel vessels. In the blank measurement both the

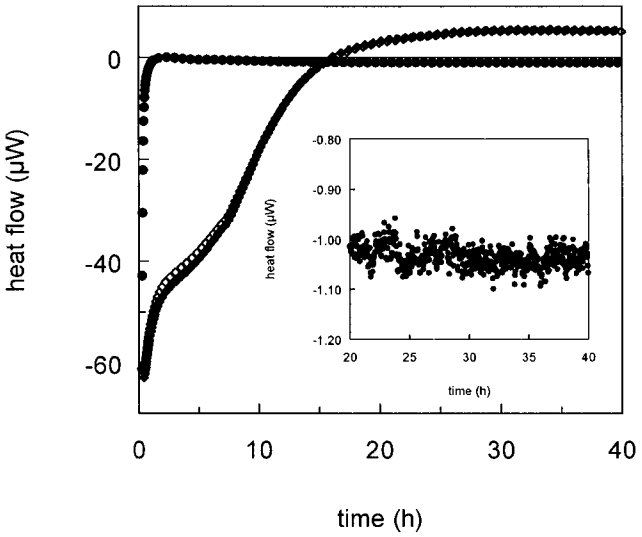

Figure 2. Typical heat flow versus time curves obtained for a blank measurement (●), with both the sample and the reference vessel filled with double-distilled water, and measurements with a 100 g/L β-lg solution (◆, ◇) in stainless steels vessels at 65.0 °C. Inset: stability of the base line. (The data points (before data reduction) of the last 20 h of the blank measurement are shown.)

sample and reference vessel were filled with double-distilled water. After introduction of the vessels into the measuring position, initially a large signal was measured due to the disturbance of the temperature equilibrium in the apparatus. The sign of this initial heat effect was either positive or negative, depending on the small temperature differences between the sample and reference vessel. After a certain time a stable and constant signal was recorded, and this signal was taken as the zero level for the experiments with β-lg. So, the apparatus was not set at zero at the beginning of each experiment, but the experiments with β-lg were corrected afterward for the zero level, determined from a blank measurement. Such blank measurements were made at each temperature, and each time the setting of the apparatus was changed. The absolute level of the blank measurements did not fluctuate much. In a time span of about 1 year the zero level did not shift more than 2 μW. Although sometimes some noise could be seen in the first hours of the blank measurement, in general a base line stability with maximum variations of less than 0.1 μW was obtained (see inset in Figure 2).

The characteristics of the measured thermograms depended very strongly on the protein concentration (see Concentration Dependence section), but some general features can be derived from the zero-corrected thermograms of 100 g/L β-lg as shown in Figure 2. All curves started with an endothermic effect, which showed that a process had started before it could be monitored. This is due to the necessary equilibration period for heating the sample. The endothermic signal decreased slowly to the zero level, crossed this level and became exothermic. This indicated that several reactions, with different heat signs and reaction rates, were occurring simultaneously.

Integration of the heat flow versus time curve to determine the net heat effect is not unambiguous. The first part of the reaction, when the reaction rate was at a maximum and thus the largest heat flow should be recorded, could not be monitored well due to the equilibration time. Although the exothermic heat flow observed in the final part of the reaction was relatively small, it lasted for a very long time. After a certain time it started to decrease, but after 3 days the zero level was still not reached. So this exothermic effect gave a significant contribution to the overall reaction heat and might be as large as the total endothermic heat effect.

TABLE 1: Core Parameter Set[a]

parameter	value
k_{diss}	1.7×10^{-4} s^{-1}
k_1	1.6×10^{-5} s^{-1}
k_2	3.5×10^{-2} mol^{-1} L s^{-1}
k_3	2.2×10^{-3} mol^{-1} L s^{-1}
Q_{diss}	−90 kJ mol^{-1}
Q_1	−90 kJ mol^{-1}
Q_2	−120 kJ mol^{-1}
Q_3	300 kJ mol^{-1}

[a] Calculated values for the rate constants and reaction heats of the dissociation, initiation, propagation, and termination reaction at 65 °C.

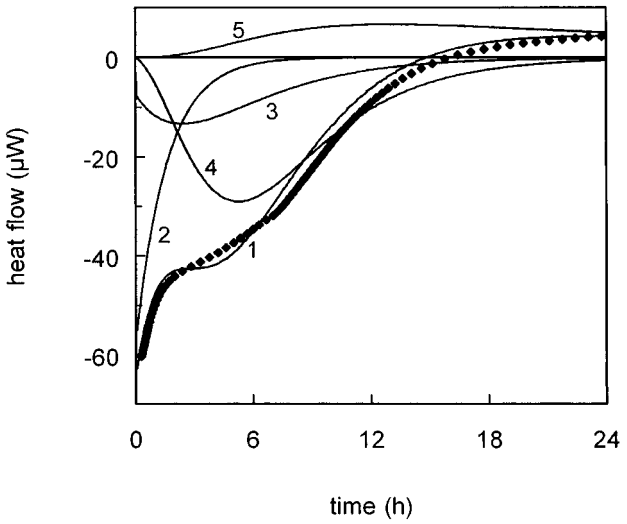

Figure 3. Experimental (◆) and calculated (line) heat flow versus time curves for 100 g/L β-lg at 65 °C. The calculated curve (1) is calculated with the parameter set given in Table 1. In addition to the total calculated heat flow versus time curve (1) also the contribution of the different reaction steps is shown: (2) dissociation; (3) initiation; (4) propagation, and (5) termination reaction.

All experiments were made at least in duplicate. As an indication of the reproducibility, two heat flow versus time curves measured for 100 g/L β-lg are shown in Figure 2. The experiments showed a very good reproducibility. In general, the same reproducibility was observed for the other concentrations, with maximum differences in absolute heat flow values of about 1 μW.

Evaluation of Core Parameter Set at 65 °C. The very pronounced shapes of the thermograms obtained with 100 g/L β-lg were used for the determination of the reaction parameters at 65 °C. In the calculations the rate constants (k_{diss}, k_1, k_2, k_3) and the reaction heats (Q_{diss}, Q_1, Q_2, Q_3) were varied in order to obtain an optimal match with the measured heat flow versus time curves. This resulted in a "best" parameter set (Table 1), considering the contributions of the different steps and requiring physically realistic and acceptable values for the rate constants and heat effects. It must be said at this point that in view of the relatively large number of parameters better fits could be found. By using information of other experiments, e.g., light-scattering and concentration determinations, we arrived at what we called the core set of parameters as presented in Table 1. The model-predicted curve in Figure 3 was calculated with this core parameter set; the contributions of the individual steps in the reaction scheme to the overall reaction heat are also shown. It then follows that the dissociation reaction contributed much to the relatively large, endothermic effect measured at the early

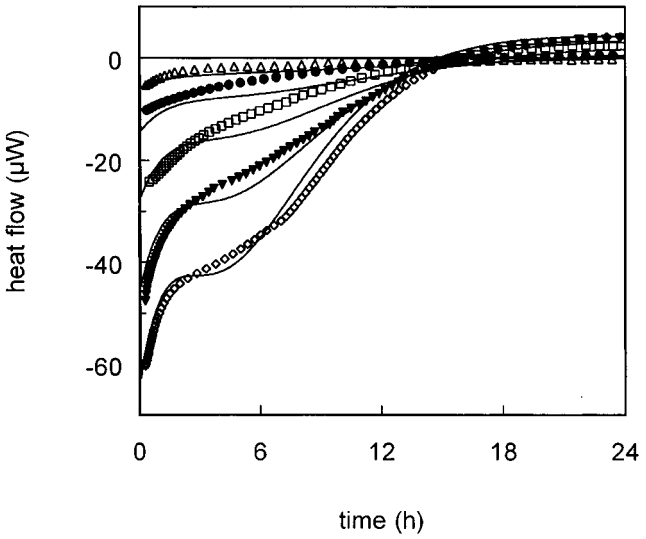

Figure 4. Experimental and calculated heat flow versus time curves at 65 °C for various β-lg concentrations: experimental data for (△) 15, (●) 30, (□) 50, (▼) 75, and (◇) 100 g/L β-lg; the calculated curves (line) were calculated with the same parameter set as in Figure 3.

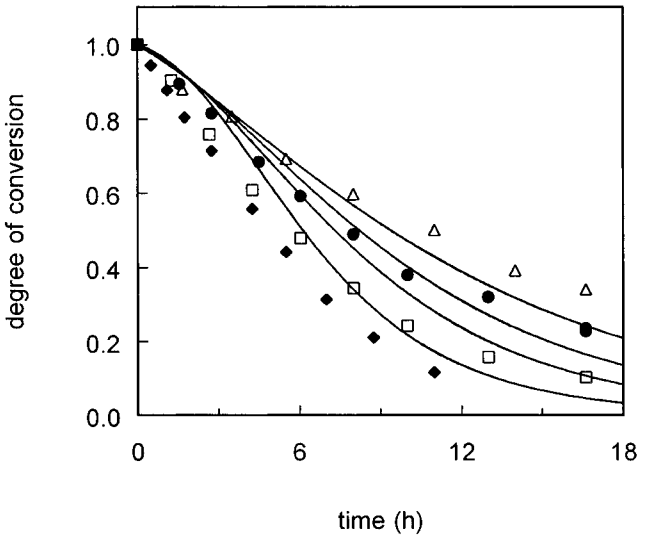

Figure 5. Experimental and calculated conversion of native β-lg as a function of time at 65 °C for various β-lg concentrations: experimental data for (△) 15, (●) 30, (□) 50, and (◆) 100 g/L β-lg; the calculated curves (line) were calculated with the core parameter set of Table 1 and as in Figure 3.

phase of the reaction and lasted for a relatively short time. The heat connected to the initiation step was relatively small whereas the propagation step determined more or less the characteristic curvature of the thermograms. The exothermic heat effect of termination reaction continued for a very long time and caused the total heat flow to become positive after longer reaction times, when the contribution of the initiation and propagation reaction had become very small.

Concentration Dependence at 65 °C. We put the core set of parameters to the test by "predicting" thermograms at different conditions. The predictive power and quality of the core parameter set were tested by measurements with various β-lg concentrations at 65 °C. The shape of the thermograms changed strongly with increasing β-lg concentration (Figure 4). For lower concentrations the heat flow approached the zero level gradually, whereas for the higher concentrations (75 and 100 g/L) after approximately 8 h a sudden change in rate occurred.

Using the core set, we calculated the thermograms for the various β-lg concentrations as indicated in Figure 4. Although the fits are certainly not perfect, they reproduce the characteristic features of the experimental curves quite satisfactorily. In particular two interesting observations can be made from Figure 4. All curves, both theoretical and experimental, crossed the zero level at the same time, after about 16 h, and the exothermic heat flow measured after that time scaled almost linearly with the initial β-lg concentration.

Further evidence for the correctness of the core parameter set was derived from the fact that this set gave a reasonable description of the experimental conversion data of Roefs and De Kruif at 65 °C (conversion of native β-lg as measured by HP-GPC).[28] Although the fit may not be optimal for all concentrations, in general a quite good agreement between the experimental data and the calculated curves can be seen (Figure 5).

We realize that other sets of parameters may exist, which give a good description of the individual experimental results, but by considering a large number of experimental results the degrees of freedom were strongly reduced. Furthermore, by extending the model through inclusion of other contributions (e.g., noncovalent (physical) aggregation and corrections for small differences in pH and salt content of the samples with different β-lg concentrations), even better fits may be obtained.

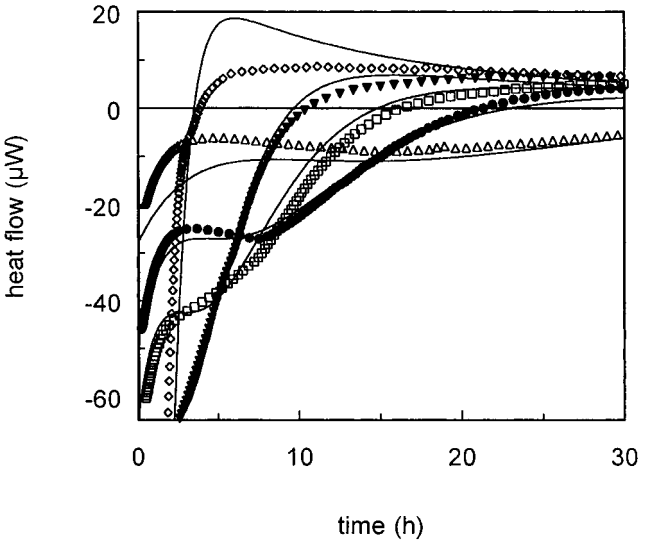

Figure 6. Experimental and calculated heat flow versus time curves for 100 g/L β-lg at various temperatures: experimental data for (△) 62, (●) 64, (□) 65, (▼) 66, and (◇) 68.5 °C. The calculated curves (line) were calculated with the core parameter set given in Table 1 for 65 °C in combination with the activation energy parameters given in table 2 for describing the temperature dependence of the rate constants of the dissociation, initiation, propagation, and termination reaction.

However, given the predictive power of our relatively simple model and the fact that with this parameter set a large number of experimental results could be described, we think that the model, in combination with the given parameter set, provides a very useful description of the experimental data.

Temperature Dependence. We tried to separate in time the underlying processes more by varying the temperature. Figure 6 summarizes the experimental and calculated thermograms for a 100 g/L β-lg solution at various temperatures. Lowering the temperature from 65 to 64 °C had already a tremendous effect on the characteristics of the thermogram. The thermograms obtained at 64 and 62 °C were much more pronounced compared with those obtained at 65 °C, indicating that several reactions were taking place at different rates. To gain more insight into the final part of the thermograms, higher temperatures were also studied. At 68.5 °C the endothermic process was accelerated

TABLE 2: Activation Energy Parameters[a]

activation energy parameter	value (kJ mol^{-1})
$E_{a,diss}$	250
$E_{a,1}$	600
$E_{a,2}$	200
$E_{a,3}$	0

[a] Temperature dependence of the rate constants. With these activation energy parameters we calculated the rate constants at temperature T using the Arrhenius equation and the core parameter set at 65 °C.

to a large extent, within 4 h the zero level was reached, and the overall reaction became exothermic. At this temperature it can be seen, as would be expected, that the exothermic heat flow reached a maximum level and then started decreasing.

From the thermograms measured at the different temperatures we derived the temperature dependence of the rate constants, using the core parameter set at 65 °C. This resulted in the activation energy values given in Table 2. The theoretical thermograms in Figure 6 were calculated with these activation energy parameters. We see that these calculated curves reproduce the essential features of the measured curves quite well. In the analysis of the temperature dependence of the rate constants of the individual processes, we noticed that the major differences in the thermograms measured at various temperatures were caused by changes in the rate of initiation step with temperature. This is reflected by the high activation energy value for this reaction step (i.e., 600 kJ/mol). This set of activation energy parameters gave also a reasonable description of the temperature-dependent shapes of the experimental curves measured for other β-lg concentrations (results not shown). Although at this moment we may have not enough information to judge whether these activation energy parameters are the true values, they enable us to describe the strongly temperature- and concentration-dependent features of the thermograms quite well. In the temperature range studied, in general a reasonable fit is obtained for all temperatures. At higher temperatures the processes occur too fast and isothermal calorimetry becomes less adequate, due to the fact that a substantial part of the reactions is already occurring during the required equilibration period and, as such, cannot be measured. At temperatures below 62 °C the signal becomes relatively small and less accurate data are obtained. So, for a kinetic investigation, temperatures in the range used in this study are the most appropriate.

Although, in view of the limited temperature range of the measurements, extrapolation of the activation energy parameters to other temperatures should be made with great care, we put this set of activation energy parameters further to the test by calculating DSC curves. Figure 7 shows a calculated and measured DSC curve for 50 g/L β-lg; the scan rate was in both cases 20 °C/h. The calculated curve resembles the experimental curve quite well. In the calculated curve the contributions of the different reaction steps are shown. At this point it may be remarked that the use of DSC for resolving the reactions involved seems of little value since, even with this low scan rate, the different processes give rise to only one (asymmetric) overall peak. Furthermore, it may be remarked that a very sensitive DSC with a highly stable base line is needed in order to detect the heat effect in the final part of the peak as an exothermic effect. Figure 8 summarizes both the measured and calculated T_p values for 50 g/L β-lg as a function of scan rate. The excellent agreement of the scan-rate dependence of the calculated and measured values gives further proof of the predictive power of this set of activation energy parameters.

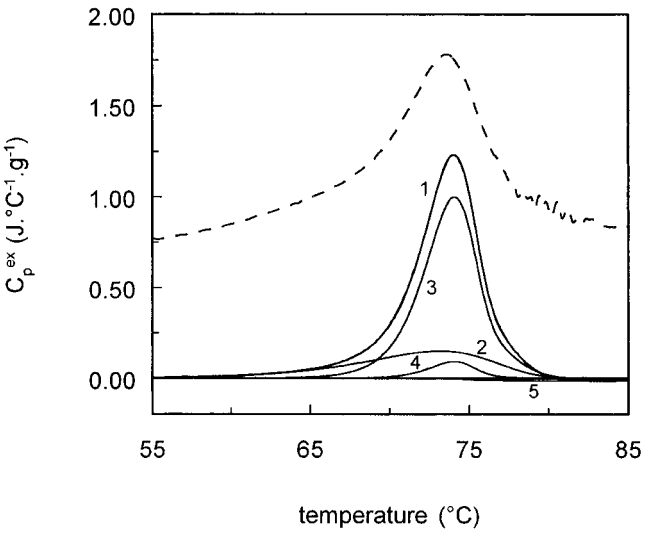

Figure 7. Experimental (dashed line) and calculated (full line, 1) DSC curve for 50 g/L β-lg, scan rate = 20 °C/h. The experimental curve was recorded with a Hart Scientific DSC 4207, and the calculated curve was calculated using the core parameter set given in Table 1 for 65 °C in combination with the activation energy parameters given in Table 2. Also, the contribution of the different reaction steps is shown: (2) dissociation; (3) initiation; (4) propagation, and (5) termination reaction.

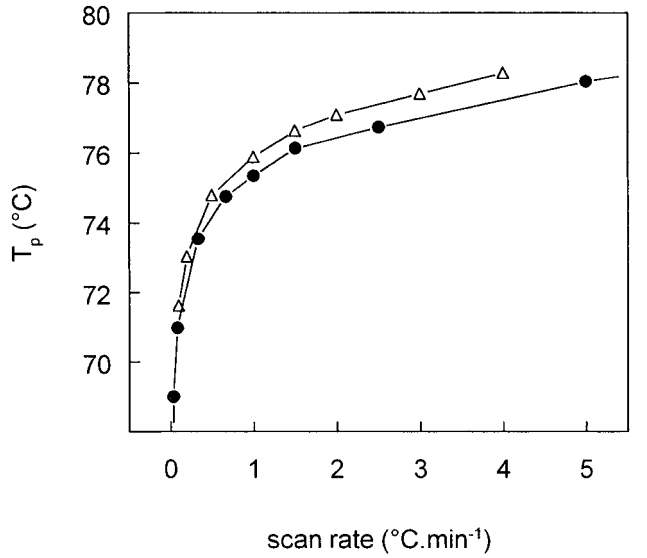

Figure 8. Experimental (●) and calculated (△) T_p values for 50 g/L β-lg as a function of scan rate. For the experimental T_p values see also Figure 1. The calculated T_p values were obtained from theoretical DSC curves, calculated for different scan rates as described in Figure 7.

Conclusions

We have shown that isothermal calorimetry offers a valuable approach to the study of the denaturation and aggregation of β-lg. It allows to unravel the processes involved more easily than does conventional DSC. The scan rates used in DSC are too high for resolving these slow processes, and the information is smeared out over the temperature traject.

The isothermal thermograms varied strongly with variations in concentration and temperature. The pronounced curves could be reproduced well using the model of Roefs and De Kruif, comprising a dissociation, initiation, propagation, and termination step.

Acknowledgment. The Thermodynamic Center Utrecht is gratefully acknowledged for kind assistance. We also thank Amaia Ariztegui Igoa for carrying out some of the experiments

and Dr. Bas Roefs for the fruitful discussions. This research was supported by the Dutch Ministry of Economic Affairs through the programme IOP-Industriële Eiwitten and by the dairy companies Coberco Research, Deventer, and Friesland Dairy Foods, Beilen.

References and Notes

(1) Mulvihill, D. M.; Donovan, M. *Ir. J. Food Sci. Technol.* **1987**, *11*, 43.
(2) Papiz, M. Z.; Sawyer, L.; Eliopoulos, E. E.; North, A. C. T.; Findlay, J. B. C.; Sivaprasadarao, R.; Jones, T. A.; Newcomer, M. E., Kraulis, P. J. *Nature* **1986**, *324*, 383.
(3) Georges, C.; Guinand, S.; Tonnelat, J. *Biochim. Biophys. Acta* **1962**, *59*, 737.
(4) Dupont, M. *Biochim. Biophys. Acta* **1965**, *102*, 500.
(5) Ptitsyn, O. B. *Adv. Protein Chem.* **1995**, *47*, 83.
(6) Iametti, S.; De Gregori, B.; Vecchio, G.; Bonomi, F. *Eur. J. Biochem.* **1996**, *237*, 106.
(7) Ma, C. Y.; Harwalkar, V. R. *Adv. Food Nutr. Res.* **1991**, *35*, 317.
(8) Park, K. H.; Lund, D. B. *J. Dairy Sci.* **1984**, *67*, 1699.
(9) Paulsson, M.; Hegg, P. O.; Castberg, H. B. *Thermochim. Acta* **1985**, *95*, 435.
(10) Qi, X. L.; Brownlow, S.; Holt, C.; Sellers, P. *Biochim. Biophys. Acta* **1995**, *1248*, 43.
(11) Relkin, P.; Launay, B. *J. Therm. Anal.* **1991**, *37*, 1887.
(12) De Wit, J. N.; Klarenbeek, G. *J. Dairy Res.* **1981**, *48*, 293.
(13) Privalov, P. L.; Khechinashvili, N. N. *J. Mol. Biol.* **1974**, *86*, 665.
(14) Privalov, P. L. *Thermochim. Acta* **1990**, *163*, 33.
(15) Hoffmann, M. A. M.; Van Mil, P. J. J. M.; De Kruif, C. G. In *Food Macromolecules and Colloids*; Dickinson, E., Lorient, D., Eds.; Royal Society of Chemistry: Cambridge, 1995; pp 171−177.
(16) Castronuovo, G. *Thermochim. Acta* **1991**, *193*, 363.
(17) Lepock, J. R.; Ritchie, K. P.; Kolios, M. C.; Rodahl, M.; Heinz, K. A.; Kruuv, J. *Biochemistry* **1992**, *31*, 12706.
(18) Sanchez-Ruiz, J. M. *Biophys. J.* **1992**, *61*, 921.
(19) Sandu, C.; Singh, R. K. *Thermochim. Acta* **1990**, *159*, 267.
(20) Hoffmann, M. A. M.; Van Miltenburg, J. C.; Van Mil, P. J. J. M. *Thermochim. Acta*, accepted for publication.
(21) Waters, D. N.; Paddy, J. L. *Anal. Chem.* **1988**, *60*, 53.
(22) Angberg, M.; Nyström, C.; Castensson, S. *Acta Pharm. Suec.* **1988**, *25*, 307.
(23) Randzio, S. L.; Suurkuusk, J. In *Biological Microbiology*; Beezer, A. E., Ed.; Academic: London, 1980; pp 311−341.
(24) Buckton, G.; Beezer, A. E. *Int. J. Pharm.* **1991**, *72*, 181.
(25) Koenigbauer, M. J. *Pharm. Res.* **1994**, *11*, 777.
(26) Kamal, M. R.; Sourour, S. *Polym. Eng. Sci.* **1973**, *13*, 59.
(27) Pusiatcioglu, S. Y.; Fricke, A. L.; Hassler, J. C. *J. Appl. Polym. Sci.* **1979**, *24*, 937.
(28) Roefs, S. P. F. M.; De Kruif, C. G. *Eur. J. Biochem.* **1994**, *226*, 883.
(29) Hoffmann, M. A. M.; Roefs, S. P. F. M.; Verheul, M.; Van Mil, P. J. J. M.; De Kruif, C. G. *J. Dairy Res.* **1996**, *63*, 423.
(30) Kelly, M. J.; Reithel, F. J. *Biochemistry*, **1971**, *10*, 2639.
(31) Zimmerman, J. K.; Barlow, G. H.; Klotz, I. M. *Arch. Biochem. Biophys.* **1970**, *138*, 101.
(32) Maubois, J. L.; Pierre, A.; Fauquant, J.; Piot, M. *IDF Bulletin* **1987**, *212*, 154.
(33) Suurkuusk, J.; Wädso, I. *Chem. Scr.* **1982**, *20*, 155.